CHARACTERIZING FADING CHANNEL UNDER ABRUPT TEMPORAL VARIATIONS

Ni-Chun Wang and Kung Yao

Electrical Engineering Department, University of California-Los Angeles, Los Angeles, USA

ABSTRACT

The statistics of the fading channel are changing due to the temporal and spatial inhomogeneity. To characterize the temporal variation of the channel, short-term statistics need to be estimated. Instead of estimating the statistics over a fixed short period, we applied the Bayesian change point detection (CPD) on the Nakagami-m channel model to capture the abrupt changes in time. The detected change points partition the channel into segments that are characterized by different parameters. We also derive the MAP estimators for the model parameters of each segment based on the hyperparameters generated by CPD. Test results on the channel measurement show the effectiveness of the CPD and the proposed estimators.

Index Terms— Fading channel, Change point detection, parameter estimation, Nakagami-m distribution

1. INTRODUCTION

Wireless channel is generally nonstationary in time, especially when the transmitters/receivers are in motion, or there are moving objects near the fixed wireless link which changes the phases of the arriving multipath signals. Therefore, the statistics or even the distribution model are changing due to the temporal and spatial inhomogeneity [1]. Studying the insight of temporal variations of the channel envelope becomes more important for wireless local area networks (WLANs) and modern mobile communications, as their transmission power is designed to be relatively low.

Several research groups have done the modeling and the analysis on the temporal variations of indoor and mobile channels causing by various conditions. In [2], it is shown that for indoor channel people moving around transmit/receive antennas causes significant temporal variation in the signal level. The human shadowing effect has been studied for a fixed wireless link under WLAN [3] and ultra-wide band (UWB) [4] indoor channels. It is shown that people moving in between the transmission path significantly changes the Rician K-factor, received power, and RMS delay spreads. In [5, 6], the authors discussed the effects of nearby traffic on the variations of Rician K-factor of outdoor urban channels. It is reported that heavy traffic causes richer scattering and thus lower K-factor. Temporal fading has also been studied for the industrial indoor environment with lots of machinery movement [7]. In [8], the first-order statistical model of the Rician K-factor was proposed, and the variations of K with time, frequency and location were also considered. In these analyses, the parameters of the probability models were estimated over a short period of observations, varying from a minute to 15 minutes. In other words, the channel samples of that fixed period were assumed to be stationary and share the same statistics.

However, the changes in the environment, such as people movement or street traffic are usually unpredictable, and the channel measurement within an interval of a few minutes could contain more than one statistical states. Estimating parameters from the whole interval may lose some insights of the true temporal variations. Hence, to precisely study the temporal variation of the channel statistics, there should be a mechanism that detects those changes. We propose using a Bayesian change point detection (CPD), which is based on the work of [9], to detect the changes in a sequence of the narrowband channel envelope samples. CPD detects sudden changes in the generative parameters of a time series. These change points naturally partition the observation into segments that are characterized by different parameters. *Maximum a posteriori* (MAP) parameter estimators are also derived based on the posterior probability generated during the CPD calculation. Hence, the channel parameters are obtained once the change points are detected.

Specifically, we focus on the Nakagami-m channel model [10]. Nakagami-m is a very flexible model covering wide range of fading scenarios through the parameter m. It is equivalent to several known distributions, such as Rayleigh and half-Gaussian, and is a very good approximation of Rice distribution [11]. Hence, by applying the CPD to the Nakagami-m model, we are able to capture the variations of statistics and also the transitions between different transmission scenarios, such as line-of-sight (LOS) and non-line-of-sight (NLOS) transmission.

2. BAYESIAN CHANGE POINT DETECTION AND EXPONENTIAL FAMILY

2.1. Bayesian Change Point Detection

The change point detection technique used here is based on the work in [9]. A brief introduction of this algorithm will be given in this section. Denote $\mathbf{h}_{1:t}$ as the data sequence, $h_1, h_2, \cdots, h_t$, observed from time 1 to t. Assume all the data are independently sampled from the same class of probability distribution, but the underlying parameter set $\boldsymbol{\theta}$ is changing over time. Consequently, the data sequence is divided into non-overlapped segments, and the data within each segment are independently sampled from the distribution of the same parameter set. A change point occurs when the parameter set changes, which is at the beginning of each segment. Define the run length r_t as the time length since the last change point observed at time t, so $r_t = 0$ indicates a change point at time t. The objective is to estimate the run length by

$$\hat{r}_t = \max_{r_t=0,1,\cdots,t} P(r_t|\mathbf{h}_{1:t}). \tag{1}$$

The posterior probability in (1) is obtained by computing the joint probability $P(r_t \cap \mathbf{h}_{1:t})$ recursively [9];

$$P(r_t \cap \mathbf{h}_{1:t}) = \sum_{r_{t-1}} P(r_t|r_{t-1})P(h_t|\mathbf{h}^{r_{t-1}})P(r_{t-1} \cap \mathbf{h}_{1:t-1}), \tag{2}$$

The work of N.-C. Wang is partially supported by National Science Council, Taiwan. (TMS-094-2-A-002).

where $\mathbf{h}^{r_{t-1}}$ denotes the data set associated with the run length r_{t-1}. Namely, the second term in (2) indicates that the current data h_t only depends on the past observations in the same run.

The modeling of the probability $P(r_t|r_{t-1})$ in (2) will be discussed in Section 3. The predictive probability $P(h_t|\mathbf{h}^{r_{t-1}})$ in (2) is associated with the data probability model through

$$P(h_t|\mathbf{h}^{r_{t-1}}) = \int P(h_t|\boldsymbol{\theta})P(\boldsymbol{\theta}|\mathbf{h}^{r_{t-1}})d\boldsymbol{\theta}, \tag{3}$$

where $P(h_t|\boldsymbol{\theta})$ is the postulated data model with parameter set $\boldsymbol{\theta}$ and is always the same class of distribution as previously mentioned. In Bayesian approach, the parameter set $\boldsymbol{\theta}$ is assumed to be random so $P(\boldsymbol{\theta}|\mathbf{h}^{r_{t-1}})$ can be viewed as the prior distribution of $\boldsymbol{\theta}$ at time t. On the other hand, the posterior probability $P(\boldsymbol{\theta}|\mathbf{h}^{r_t})$ obtained by normalizing the integrand in (3) will be served as the prior at time $t+1$. If there exists a prior that is *conjugate* to the data model, the resulting posterior probability is still in the same class of distribution as the prior. Consequently, the integrand in (3) will always be in a fixed form if the conjugate prior is applied, greatly reducing the computational complexity of evaluating (3).

2.2. Exponential Family and Conjugate Prior

It is known the distribution models in the exponential family must have conjugate priors [12]. Fortunately, the common models of the fading channel envelope, such as Rayleigh, Nakagami-m, and Weibull distribution, are exponential families. The distribution of a random variable X with parameter set $\boldsymbol{\theta}$ belongs to an exponential family if the probability density function (pdf) can be written as

$$P(x|\boldsymbol{\theta}) = b(x)g(\boldsymbol{\theta})\exp\left(\boldsymbol{\phi}(\boldsymbol{\theta})^T\mathbf{u}(x)\right), \tag{4}$$

where $b(x)$ and $g(\boldsymbol{\theta})$ are known functions, and $\boldsymbol{\phi}(\boldsymbol{\theta})$ and $\mathbf{u}(x)$ are vectors of the same dimension as that of $\boldsymbol{\theta}$. The prior of $\boldsymbol{\theta}$ conjugate to (4) has to be proportional to [12]

$$P(\boldsymbol{\theta}) \propto g(\boldsymbol{\theta})^\gamma \exp\left(\boldsymbol{\phi}(\boldsymbol{\theta})^T\boldsymbol{\nu}\right), \tag{5}$$

with the hyperparameter set $\boldsymbol{\eta} = \{\gamma, \boldsymbol{\nu}\}$. In the following sections we will use (5) to find the conjugate prior of the distributions of interest. Additionally, it can be easily proved that $\boldsymbol{\theta}$ depends on x only through the hyperparameter set $\boldsymbol{\eta}$. Hence, $\boldsymbol{\eta}$ is the *sufficient statistic* for $\boldsymbol{\theta}$, and $P(\boldsymbol{\theta}|x) = P(\boldsymbol{\theta}|\boldsymbol{\eta})$. As observing more data, we should update the posterior probability through updating the sufficient statistic.

3. CPD AND PARAMETER ESTIMATION FOR NAKAGAMI-M FADING CHANNEL

In this section, we will discuss how to apply the change point detection theory introduced in Section 2 on Nakagami-m fading channel model. The pdf of an Nakagami-m random variable h is written as

$$f(h|m,\Omega) = \frac{2}{\Gamma(m)}\left(\frac{m}{\Omega}\right)^m h^{(2m-1)}e^{-\frac{mh^2}{\Omega}},\ h \geq 0, \tag{6}$$

where Ω is the expected second moment of h_t. The parameter m ($m \geq 1/2$) indicates the level of fading. For $m = 1$, (6) is equivalent to a Rayleigh pdf. For $m > 1$, (6) is a good approximation of a Rice pdf where m is proportional to the Rician K-factor.

To apply the Nakagami-m chanel model to the Bayesian change point detection algorithm, the conjugate prior needs to be found. First, we replace the parameter $1/\Omega$ with γ for the convenience of the future derivations. Follow (4), the Nakagami-m pdf consists of

$$b(h_t) = 2,\ g(m,\gamma) = \frac{1}{\Gamma(m)}(m\gamma)^m, \tag{7}$$

$$\boldsymbol{\phi}(m,\gamma) = [-m\gamma\ \ 2m-1]^T,\ \mathbf{u}(h_t) = \left[h_t^2\ \ \ln h_t\right]^T. \tag{8}$$

Consequently, using (5) the conjugate prior is in the form of

$$P(m,\gamma|n,\nu,s,p) \propto \frac{1}{\Gamma^n(m)}(m\gamma)^{\nu m}p^{2m-1}\exp\{-ms\gamma\}, \tag{9}$$

with hyperparameter set $\boldsymbol{\eta} = \{n,\nu,s,p\}$. There is no known distribution in the exponential family with pdf in the form of (9). However, it is not difficult to find the normalization constant of (9) by numerical integration. Let K be the normalization constant, which is a function of $\boldsymbol{\eta}$. Namely,

$$K(\boldsymbol{\eta}) = \int_m\int_\gamma \frac{1}{\Gamma^n(m)}(m\gamma)^{\nu m}p^{2m-1}\exp\{-ms\gamma\}\,d\gamma dm. \tag{10}$$

It is observed that the conditional pdf $f(\gamma|m)$ can be written into a gamma distribution, so $K(\boldsymbol{\eta})$ can be simplified to

$$\int_m\int_\gamma \underbrace{\frac{(ms)^{\nu m+1}}{\Gamma(\nu m+1)}\gamma^{(\nu m+1)-1}e^{-ms\gamma}}_{f(\gamma|m)}d\gamma\frac{\Gamma(\nu m+1)}{ms^{\nu m+1}}\frac{p^{2m-1}}{\Gamma^n(m)}dm$$

$$= \int_{1/2}^{\infty}\frac{\Gamma(\nu m+1)}{\Gamma^n(m)}\frac{p^{2m-1}}{ms^{\nu m+1}}dm. \tag{11}$$

To find K, we applied the Laplace's method [13], in which the integrand is approximated by a Gaussian pdf. Suppose we would like to find $\int_x f(x)dx$ for some given function $f(x)$. Let $q(x) = \ln f(x)$ and $x^* = \max_x q(x)$. The idea of the Laplace's method is to approximate $f(x)$ by $\exp\{\hat{q}(x)\}$, where $\hat{q}(x)$ is the second-order Taylor's approximation of $q(x)$ around x^*. Hence, the integral of interest is approximated by $\int_x \exp\{\hat{q}(x)\}\,dx$, which yields

$$f(x^*)\sqrt{2\pi/|q''(x^*)|}\int_x \mathcal{N}\left(x;x^*,1/|q''(x^*)|\right)dx. \tag{12}$$

The integrand in (12) is a Gaussian pdf with the mean x^* and the variance $\frac{1}{|q''(x^*)|}$. The integral of a Gaussian pdf can be expressed by the Q-function, which is defined as $Q(x) = \int_x^\infty 1/\sqrt{2\pi}e^{-t^2/2}dt$ and can be easily approached by numerical approximation. Hence, to apply the Laplace's method, one only needs to find $q''(x)$ and x^*.

Using Laplace's method to find K in (11), first we define $q(m)$ as the logarithm of the integrand in (11). The second derivative of $q(m)$ is

$$q''(m) = \nu^2\psi^{(1)}(\nu m+1) - n\psi^{(1)}(m) + m^{-2}, \tag{13}$$

where $\psi^{(k)}(m)$ is the polygamma function defined as the $(k+1)^{\text{th}}$ derivative of the logarithm of the gamma function. From (12) and (13), $K(\boldsymbol{\eta})$ can be approximated by

$$\frac{\Gamma(\nu m^*+1)}{\Gamma^n(m^*)}\frac{p^{2m^*-1}}{ms^{\nu m^*+1}}\sqrt{\frac{2\pi}{|q''(m^*)|}}Q\left(\frac{\frac{1}{2}-m^*}{\sqrt{1/|q''(m^*)|}}\right). \tag{14}$$

Therefore, m^*, the m that maximizes $q(m)$, is the only thing left we need to solve. To find m^*, we set $q'(m)$ to zero; namely

$$q'(m^*) = \nu\psi^{(0)}(\nu m^*+1) - n\psi^{(0)}(m^*) - \frac{1}{m^*} + \ln\frac{p^2}{s^\nu} = 0. \tag{15}$$

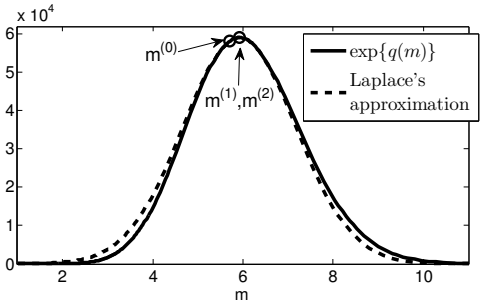

Fig. 1. An example of using Laplace's approximation for the integrand in (11). $m^{(k)}$ denotes the result of k^{th} iteration of Newton's method for searching m^* and $m^{(0)}$ is the initial value.

From [14], it is shown that $\psi^{(0)}(m)$ can be approximated by

$$\psi^{(0)}(m) = \ln(m) - \frac{1}{2m} - \frac{1}{12m^2} + \frac{1}{120m^4} - \frac{1}{252m^6} + O\left(\frac{1}{m^8}\right). \tag{16}$$

By only taking the first term in the series above and ignoring $1/m^*$ in (15), we can find a crude estimate of $m^* \approx \left(\frac{s}{\nu p^{2/\nu}}\right)^{\frac{\nu}{\nu-n}}$. Take this estimate as a initial point and perform Newton's method, we can find a more accurate m^*. In Fig. 1, an example of using Laplace's approximation for the original integrand $\exp\{q(m)\}$ is shown. In this example, the parameters of $q(m)$ are set to $n = 10,\ \nu = 7,\ s = 5$, and $p = 3$. The original integrand $\exp\{q(m)\}$ is fairly close to a Gaussian bell shape, so $\exp\{\hat{q}(m)\}$ leads a good approximation. The results of the Newton's method for searching m^* are also shown in the figure,where $m^{(k)}$ is the result of k^{th} iteration and $m^{(0)}$ is the initial value. In this example, the Newton's method converges in only two iterations since the initial estimate is close to the true m^*.

With $K(\boldsymbol{\eta})$ and the conjugate prior form in (9), we are able to derive the predictive probability using (3), which yields

$$P(h_t|\mathbf{h}^{r_{t-1}}) = \frac{2K(\boldsymbol{\eta}^{r_t})}{K(\boldsymbol{\eta}^{r_{t-1}})}, \tag{17}$$

where $\boldsymbol{\eta}^{r_t}$ is the hyperparameter set updated by the observations $\mathbf{h}^{r_t}$. Also, since the posterior probability resulting from the integrand in (3) is still in the same distribution form as the conjugate prior, by comparing the hyperparameter sets in the posterior and in the prior, we can easily obtain the updating equations for the hyperparameter set $\boldsymbol{\eta}^{r_t}$,

$$\begin{aligned} n^{r_t} &= n^{r_{t-1}} + 1, \ \ \nu^{r_t} = \nu^{r_{t-1}} + 1, \\ p^{r_t} &= p^{r_{t-1}} \cdot h_t, \ \ s^{r_t} = s^{r_{t-1}} + h_t^2. \end{aligned} \tag{18}$$

Hence, when observing a new sample h_t, we first update the hyperparameters using (18) and then plug the updated hyperparameter set into (17) to obtain the new predictive probability.

Besides the predictive probability, the run length transition probability $P(r_t|r_{t-1})$ needs to be defined in order to use (2). Given r_{t-1}, r_t could only be 0 or $r_{t-1}+1$. Hence, the run length transition probability is fully defined by $P(r_t = 0|r_{t-1})$. Since the change points of the fading channel occurs randomly, we simply take $P(r_t = 0|r_{t-1}) = 1/\lambda$ which indicates that a change point occurs at time t does not depend on the previous run length. The constant λ is the expected length of each segment, which should be tuned for different transmission environments. This is also equivalent of assuming the length of each segment follows a geometric distribution with mean λ.

3.1. MAP parameter estimators

We estimate the parameters of the Nakagami-m pdf based on the observations in the current segment $\mathbf{h}^{r_t}$ by MAP criterion. Since the conjugate prior is used, the posterior probability $P(m, \gamma|\mathbf{h}^{r_t})$ is also in the same form as in (9),

$$P(m, \gamma|\mathbf{h}^{r_t}) = \frac{(m\gamma)^{\nu^{r_t} m} \left(p^{r_t}\right)^{2m-1}}{K(\boldsymbol{\eta}^{r_t})\Gamma^{n^{r_t}}(m)} \exp\left\{-s^{r_t} m\gamma\right\}. \tag{19}$$

First we take the partial derivative of the logarithm of $P(m, \gamma|\mathbf{h}^{r_t})$ with respect to γ and set to 0, and the MAP estimator of γ corresponding to the estimated run length $\hat{r}_t$ can be easily solved,

$$\gamma_t^{\text{MAP}} = \frac{\nu^{\hat{r}_t}}{s^{\hat{r}_t}}. \tag{20}$$

Note that the MAP estimator of Ω is not $1/\gamma_t^{\text{MAP}}$ since the MAP estimator does not commute over nonlinear transformations [15].

On the other hand, by setting $\partial \ln P(m, \gamma|\mathbf{h}^{r_t})/\partial m = 0$ and plugging in the MAP estimator of γ, we obtain

$$\ln m - \frac{n^{r_t}}{\nu^{r_t}} \psi^{(0)}(m) = \ln \frac{s^{r_t}}{\nu^{r_t} \left(p^{r_t}\right)^{2/\nu^{r_t}}}. \tag{21}$$

Apply the approximation in (16) and preserve the first three terms of the series, the equation (21) becomes

$$\left(1 - \frac{n^{r_t}}{\nu^{r_t}}\right) \ln m + \frac{1}{2m} + \frac{1}{12m^2} = \ln \frac{s^{r_t}}{\nu^{r_t} \left(p^{r_t}\right)^{2/\nu^{r_t}}}. \tag{22}$$

m_t^{MAP} can be solved from (22) by numerical methods. A faster but less accurate way to approach m_t^{MAP} is by observing from (18) that $\lim_{r_t \to \infty} \frac{n^{r_t}}{\nu^{r_t}} = 1$ when the initial values of n and ν are fairly close, so that (22) can be simplified to a quadratic equation. Consequently, the MAP estimator corresponding to $\hat{r}_t$ is a root of the quadratic equation, which has a closed-form expression

$$m_t^{\text{MAP}} = \frac{6 + \sqrt{36 + 48C^{\hat{r}_t}}}{24C^{\hat{r}_t}}, \tag{23}$$

where $C^{\hat{r}_t} = \ln s^{\hat{r}_t}/\nu^{\hat{r}_t} \left(p^{\hat{r}_t}\right)^{2/\nu^{\hat{r}_t}}$. Note that the other root is invalid since it is negative. The estimator in (23) is accurate as we collect more data from the same segment such that $\frac{n^{r_t}}{\nu^{r_t}}$ is close to 1. Also, it is known from the estimation theory that the MAP estimator converges to maximum likelihood (ML) estimator as the number of observations grows large [15]. Our MAP result in (23) indeed converges to the ML estimator derived in [16].

4. EVALUATION

To validate the CPD methods and parameter estimators for the Nakagami-m distribution, we first test with the Nakagami-m pseudo random sequence generated by Matlab. The sequence is manually partitioned into 4 non-overlapped segments. The samples within each segment are independent and identically distributed. The parameters for each segment are are $m = \{1, 2, 4, 3\}$ and $\gamma = \{1, 1.42, 0.83, 1.33\}$. As previously discussed, the generated random sequence simulates the scenario when the transmission is turning from NLOS ($m = 1$) to LOS ($m > 1$).

Fig. 2 shows the CPD and parameter estimation results. The true change points are at $t = \{251, 551, 751\}$ and the estimated change point are at $t = \{262, 551, 751\}$. The first detected change point is slightly behind the true one because the first few samples of the

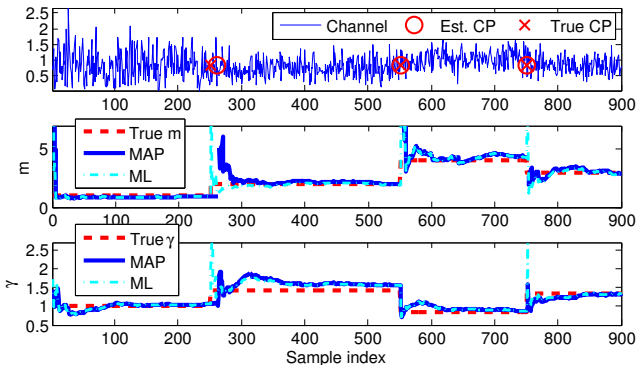

Fig. 2. Results of the CPD on a Nakagami-m random sequence with 4 segments. The sequential MAP estimators of m and γ are shown in the second and third subplots, respectively.

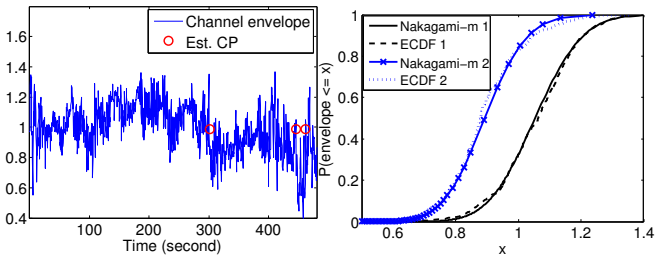

(a) (b)

Fig. 3. (a) CPD results on the channel measurement of the first scenario. (b) Comparison between the empirical CDFs of the first two detected segments and the corresponding Nakagami-m CDFs using the estimated parameters.

second segment have closer statistics to the one of the first segment. For comparison, we also show the sequential ML estimator in the same figure. Note that this sequential ML estimator is computed based on the full knowledge of the change point locations and thus can be viewed as one of the best statistical estimators if the change point locations are provided. The ML estimators for m and γ were derived in [16]. For both m and γ, our MAP estimators depending on the detected change point locations perform very closely to the ML estimator, especially after observing more data in the same segment.

Next, we test the proposed method on the channel measurement. The experiment was conducted in a lab room, which is surrounded by wooden walls and glasses windows. Both transmitter and receiver are the radio module SC2000 by Silvus Technologies. The carrier frequency is 2.49 GHz. In practice, the channel samples are time correlated, which violates the independence assumption in the CPD and the parameter estimator. As pointed out in [2, 5, 6], as the channel sampling interval increases, the temporal correlation between samples drops rapidly and can be viewed as "approximately independent". In each experiment, the channel was measured for 8 minutes with 0.48 second sampling interval which is long enough for independent assumption. The transmitter and the receiver were fixed and separated by 3.2 meters at all time during the measurement. The time average power of the channel envelope in each experiment was normalized to 1.

In the first scenario, there was a no object in between the transmission path. Four prearranged people were walking nearby the receiver. As reported in [2], people moving around the receiver would

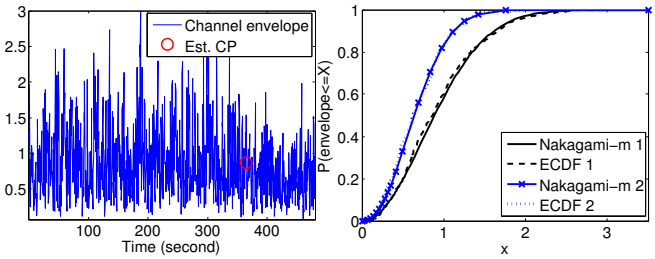

(a) (b)

Fig. 4. (a) CPD results on the channel measurement of the second scenario. (b) Comparison between the empirical CDFs of the two detected segments and the corresponding Nakagami-m CDFs using the estimated parameters.

cause larger variation in the Rician K-factor than people moving around the transmitter. The results of applying Nakagami-m CPD on the measurement are shown in Fig. 3(a). There are 4 detected segments and 3 change points at $t = \{300.96, 445.92, 461.28\}$ seconds respectively. For each segment, we take the MAP estimation of m and γ from the last time instant of the estimated segment. The number of sample points in the last two estimated segments are relatively small, so we only consider the goodness-of-fit for the first two segments. The MAP estimated $\{m, \gamma\}$ are $\{19.9613, 0.8864\}$ and $\{17.7114, 1.2319\}$ for the two segments, respectively. Using those estimated parameters, the two estimated Nakagami-m cumulative distribution functions (CDF) (denoted as Nakagami-m 1 and 2) and the corresponding empirical CDF (denoted as ECDF 1 and 2) of the two segments are plotted in Fig. 3(b). It is clear that the distributions of the two segments are significantly different. Using the Komolgorov-Smirnov goodness-of-fit test (KS test) [17], both cases pass the test under the significance level 1%. Also, from the estimated m values, the equivalent Rician K-factor are over 30 for both cases, which matches the experiment setting since there was a clear LOS between antennas.

In the second scenario, people were consistently walking or standing still in between the transmitter and the receiver. Therefore, there was no direct sight between antennas at most of the time. The results of the CPD are shown in Fig. 4(a). One change point is detected at 364.8 second. The MAP estimated $\{m, \gamma\}$ are $\{1.0021, 0.8821\}$ and $\{1.1377, 1.7724\}$ for the two segments, respectively. The comparison between the empirical CDFs of the segments and their corresponding Nakagami-m CDFs is shown in Fig. 4(b). Both cases pass the KS test with a significance level 1%. The estimated m of both segment are very close to 1 which implies there is a strong multipath fading effect and the envelope distribution is also close to a Rayleigh.

5. CONCLUSION

We proposed a precise way to characterize the abrupt temporal variations in the wireless fading channel. Applying Nakagami-m CPD can provide us the variations of the fading condition and the power of the channel envelope. The MAP parameter estimation can be obtained directly from the hyperparameter sets of the conjugate prior. CPD combining with parameter estimation can give us a more accurate view of modeling the empirical channel data. This is useful especially for the indoor measurement as in our experiment, since the channel envelope usually suffers from human shadowing and has larger temporal variations.

6. REFERENCES

[1] H. Hashemi, "The indoor radio propagation channel," *Proceedings of the IEEE*, vol. 81, no. 7, pp. 943–968, Jul. 1993.

[2] H. Hashemi, M. McGuire, T. Vlasschaert, and D. Tholl, "Measurements and modeling of temporal variations of the indoor radio propagation channel," *IEEE Transactions on Vehicular Technology*, vol. 43, no. 3, pp. 733–737, Aug. 1994.

[3] P. Hafezi, A. Nix, and M. Beach, "An experimental investigation of the impact of human shadowing on temporal variation of broadband indoor radio channel characteristics and system performance," in *Vehicular Technology Conference, 2000. IEEE VTS-Fall VTC 2000. 52nd*, vol. 1, 2000, pp. 37–42.

[4] P. Pagani and P. Pajusco, "Experimental assessment of the UWB channel variability in a dynamic indoor environment," in *15th IEEE International Symposium on Personal, Indoor and Mobile Radio Communications, 2004. PIMRC 2004*, vol. 4, Sep. 2004, pp. 2973–2977.

[5] L. Ahumada, R. Feick, R. Valenzuela, and C. Morales, "Measurement and characterization of the temporal behavior of fixed wireless links," *IEEE Transactions on Vehicular Technology*, vol. 54, no. 6, pp. 1913–1922, Nov. 2005.

[6] L. Ahumada, R. Feick, and R. Valenzuela, "Characterization of temporal fading in urban fixed wireless links," *IEEE Communications Letters*, vol. 10, no. 4, pp. 242–244, Apr. 2006.

[7] E. Tanghe, W. Joseph, L. Verloock, L. Martens, H. Capoen, K. Van Herwegen, and W. Vantomme, "The industrial indoor channel: large-scale and temporal fading at 900, 2400, and 5200 MHz," *IEEE Transactions on Wireless Communications*, vol. 7, no. 7, pp. 2740–2751, Jul. 2008.

[8] L. Greenstein, S. Ghassemzadeh, V. Erceg, and D. Michelson, "Ricean k-factors in narrow-band fixed wireless channels: Theory, experiments, and statistical models," *IEEE Transactions on Vehicular Technology*, vol. 58, no. 8, pp. 4000–4012, Oct. 2009.

[9] R. P. Adams and D. J. C. MacKay, "Bayesian online changepoint detection," *Technical Report, University of Cambridge*, Oct. 2007. [Online]. Available: http://arxiv.org/abs/0710.3742

[10] M. Nakagami, "The m-distribution-a general formula of intensity distribution of rapid fading," *Statistical Method of Radio Propagation*, 1960.

[11] R. Vaughan, J. Bach-Anderson, and J. B. Andersen, *Channels, Propagation and Antennas for Mobile Communications*. IET, 2003.

[12] A. Gelman, J. Carlin, H. Stern, and D. Rubin, *Bayesian Data Analysis, Second Edition*. Chapman and Hall/CRC, Jul. 2003.

[13] L. Tierney and J. B. Kadane, "Accurate approximations for posterior moments and marginal densities," *Journal of the American Statistical Association*, vol. 81, no. 393, p. 82, Mar. 1986.

[14] J. M. Bernardo, "Algorithm AS 103: Psi (Digamma) function," *Applied Statistics*, vol. 25, no. 3, p. 315, 1976.

[15] S. M. Kay, *Fundamentals of Statistical Signal Processing: Estimation Theory*. Prentice-Hall PTR, 1993.

[16] J. Cheng and N. Beaulieu, "Maximum-likelihood based estimation of the Nakagami-m parameter," *IEEE Communications Letters*, vol. 5, no. 3, pp. 101–103, Mar. 2001.

[17] D. Sheskin, *Handbook of Parametric and Nonparametric Statistical Procedures*. CRC Press, 2004.